Observation of surface ferromagnons in the axion-insulating phase of the antiferromagnetic topological insulator $EuSn_2As_2$

Mamoun Hemmida,[1,*] Santanu Pakhira,[2,3] David C. Johnston,[2,4] and Hans-Albrecht Krug von Nidda[1,†]

[1]*Experimental Physics V, Center for Electronic Correlations and Magnetism, University of Augsburg, D-86135 Augsburg, Germany*

[2]*Ames National Laboratory, Iowa State University, Ames, Iowa 50011, USA*

[3]*Institute for Quantum Materials and Technologies, Karlsruhe Institute of Technology, D-76021 Karlsruhe, Germany*

[4]*Department of Physics and Astronomy, Iowa State University, Ames, Iowa 50011, USA*

(Received 26 September 2023; revised 23 February 2024; accepted 9 May 2026; published 17 June 2026)

We report the study of spin dynamics of Eu^{2+} in the antiferromagnetic axion topological insulator $EuSn_2As_2$ by means of antiferromagnetic resonance at 9.34 GHz. Below the Néel temperature (T_N), two types of resonance modes, the conventional bulk antiferromagnetic resonance and additional surface ferromagnetic resonance, are observed. The latter turns out to be characteristic of the axion-insulating phase. Above T_N, we prove the existence of a Kosterlitz-Thouless scenario that is relevant for the spin relaxation in the Eu^{2+} layers. The absence of Korringa relaxation indicates the strong confinement of the conduction electrons at the Fermi level to the SnAs layers.

DOI: 10.1103/dp4g-dyll

I. INTRODUCTION

An axion is a hypothetical particle that was suggested in 1977 by postulating a new U(1) symmetry, in order to solve the strong charge-parity problem of quantum chromodynamics (QCD) in the standard model (SM) of elementary particles [1–4]. This was achieved by adding a pseudoscalar field, the so-called axion field ϑ_{QCD}, to the SM Lagrangian: $\mathcal{L}_{SM} \propto \vartheta_{QCD} G^a_{\mu\nu} \tilde{G}^{a\mu\nu}$, where $G^a_{\mu\nu} = 1, 2, \ldots, 8$ are the field strength tensors in the theory of QCD. In condensed matter physics, in order to provide a simple understanding of the anomaly of the currents and the fractional electric charge in the PbTe-type narrow-gap semiconductors, the axion field ϑ_{CM} is introduced into the ordinary electromagnetic Lagrangian as $\mathcal{L}_{EM} \propto \vartheta_{CM} \mathbf{E} \cdot \mathbf{B}$, where $\mathbf{E}$ and $\mathbf{B}$ are the electric and magnetic fields, respectively [5,6].

Theoretical studies of the antiferromagnetic topological insulator $BiFe_2Se_3$ [7] proposed a new type of polariton (axionic polariton), which is the coupled mode of light and the axionic mode of an antiferromagnet. Optical magnetoelectric resonance measurements at terahertz frequencies found an axion-type coupling in the polar magnet $(Fe, Zn)_2Mo_3O_8$ [8]. Among antiferromagnetic topological materials, bulk three-dimensional topological insulators show a quantized topological magnetoelectric effect, which is a hallmark of axion topological insulators [9–13]. Commonly, the description of the basic properties of static and dynamical axion insulators requires magnetic order [14]. Indeed, an axion phase was discovered in the layered van der Waals antiferromagnet $MnBi_2Te_4$ with an A-type magnetic structure with the Mn moments aligned along the trigonal c axis [15–22]. This compound belongs to the $(MnBi_2Te_4)(Bi_2Te_3)_n$ family, which reflects the interplay between the topology of the electronic structure and spontaneous symmetry breaking [23–27]. Currently, new axion topological insulators, the so-called Zintl-phase compounds $EuSn_2As_2$, $EuIn_2P_2$, $EuIn_2As_2$, and $EuSn_2P_2$, show that the evolution of Dirac surface states is induced by magnetic order [23,28–36]. The magnetic-order effect is attributed to the hybridization between the localized magnetic moments from either $4f$ or $3d$ orbitals and the topological electronic states.

$EuSn_2As_2$ crystallizes in the layered $NaSn_2As_2$-type crystal structure with trigonal space group $R\bar{3}m$ [37–39]. The Eu^{2+} ions ($4f^7; S = 7/2$) form a hexagonal unit cell in the ab plane. The Eu layers are stacked alternately and each Eu atom is coordinated by six As atoms to form a trigonal prism. The Sn and As atoms are covalently bonded in a honeycomb arrangement and the Sn atoms between two adjacent Sn-As layers face each other with inversion symmetry. The system exhibits van der Waals layered character with a collinear A-type antiferromagnetic order along the c axis below $T_N \approx 24$ K (see the Supplemental Material [40]). Eu^{2+} magnetic moments are aligned ferromagnetically in the ab plane, with an easy-plane anisotropy character [38].

In this work, we provide evidence for the existence of surface ferromagnons in the axion phase of $EuSn_2As_2$, by probing the spin dynamics of Eu^{2+} by means of electron spin resonance (ESR). Moreover, the isostructural antiferromagnetic topological insulator $EuAl_2Ge_2$ is studied as a reference compound to work out the specific axion-related magnetic resonance properties of $EuSn_2As_2$ (see the Supplemental Material [40]). Above T_N, the spin correlations

*Contact author: Mamoun.hemmida@physik.uni-augsburg.de
†Contact author: Hans-albrecht.krug@physik.uni-augsburg.de

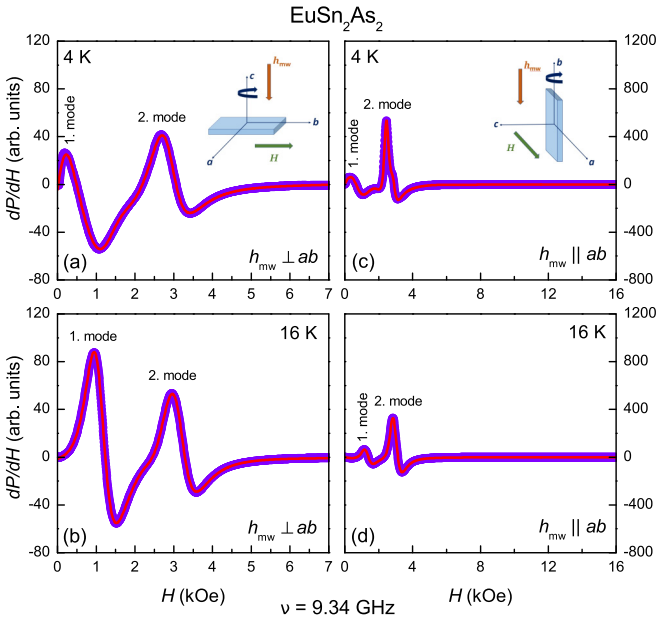

FIG. 1. Selected antiferromagnetic resonance spectra of $EuSn_2As_2$ are taken corresponding to Figs. 2(a) and 2(b) and Figs. 2(c) and 2(d) at 4 and 16 K, respectively. Both first and second magnon modes are well described by red Dysonians. The two sketches in the insets of panels (a) and (c) show the different positions of the sample in the resonance cavity with respect to the static field H and microwave field $h_{\rm mw}$, where $H \perp h_{\rm mw}$.

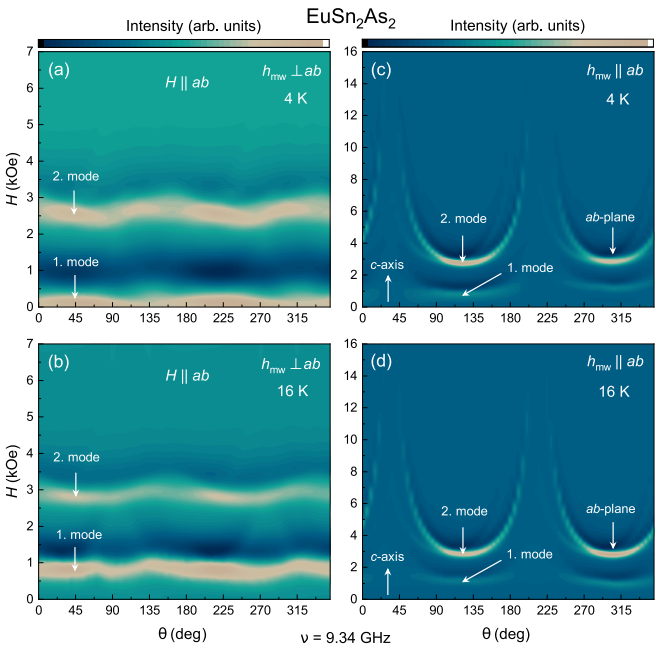

FIG. 2. Microwave absorption of $EuSn_2As_2$ as a function of angle and magnetic field H up to 16 kOe at selected temperatures. By applying $h_{\rm mw} \perp ab$ and $h_{\rm mw} || ab$, two resonance modes are observed. The second magnon mode appears very close to the paramagnetic resonance line, while the first one shifts to higher resonance fields as temperature increases.

are assigned to a Berezinskii-Kosterlitz-Thouless (BKT) scenario [41–43]. For $T > 100$ K, the strong confinement of conduction electrons marks the ideal topological insulating phase.

II. EXPERIMENTAL DETAILS

$EuSn_2As_2$ single crystals were grown as described in Ref. [38]. Temperature- and angular-dependent antiferromagnetic resonance experiments were performed using a continuous-wave ESR spectrometer (Bruker ELEXSYS E500A) at X-band frequency for in- and out-of-plane sample adjustments. The crystals were fixed in quartz tubes with paraffin. Using a continuous helium gas-flow cryostat ESR 900 (Oxford Instruments), the measurements were carried out for $4\,\text{K} \leqslant T \leqslant 300\,\text{K}$. The orientation of the samples was controlled by a programmable goniometer in 5° steps during a full rotation. The signal was detected at constant excitation frequency in a resonant cavity by sweeping the applied static magnetic field H up to 16 kOe. The microwave field $h_{\rm mw}$ remains always perpendicular to H, which detects only the transverse magnons. The signal-to-noise ratio was improved by means of lock-in technique with field modulation. Hence, one obtains the field derivative of the absorbed microwave power as depicted in Fig. 1, where typical ESR spectra of the antiferromagnetic phase are shown for two excitation geometries and at two temperatures.

III. EXPERIMENTAL RESULTS AND DISCUSSIONS

In the antiferromagnetic phase of $EuSn_2As_2$, due to the weak interlayer coupling, and strong easy-plane anisotropy and exchange field, a small antiferromagnetic gap is expected. Indeed, two different magnon modes have been observed within the range of X band. The second mode remains nearly constant and close to the paramagnetic resonance field value $H_{\rm res.} \approx 3.4$ kOe, while the first mode shifts to lower $H_{\rm res.}$ as temperature decreases (Figs. 1 and 2). Both modes are well described by the field derivative of a Dysonian, i.e., a Lorentzian including a certain contribution of dispersion besides the absorption due to the metallic conductivity of the sample. Only for the magnetic field applied within the ac plane, slight distortions of the signals show up at lowest temperatures, which can be taken account by a weak second Dysonian and result from local demagnetization effects. Note that the first mode exhibits practically the same amplitude for the microwave field applied parallel or perpendicular to the crystallographic c axis, while the amplitude of the second mode is much stronger for the latter case.

The full angular dependence for both rotation geometries is depicted in Fig. 2, where the color-coded amplitude of Fig. 1 is plotted as a function of angle and magnetic field. Within the ab plane, there is no significant angular dependence except for a weak 180° modulation due to a slight tilting of the c axis with respect to the rotation axis. Regarding the ac plane, the resonance field of the second mode exceeds the accessible field range of our electromagnet for the magnetic field applied along the c axis in agreement with the significant easy-plane anisotropy known from magnetization measurements. The

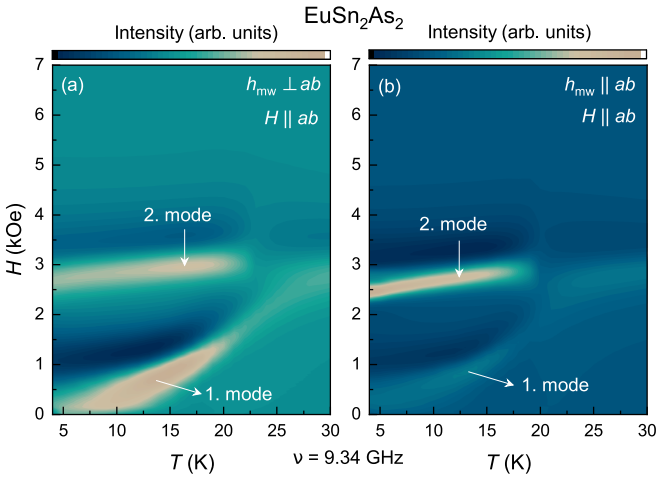

FIG. 3. Microwave absorption of $EuSn_2As_2$ as a function of temperature for (a) out-of-plane and (b) in-plane applied magnetic microwave fields, respectively. The first mode approaches the second one for $T \geqslant T_N$.

first mode also shifts to higher fields, but fades out for $H||c$. Note that the reference compound $EuAl_2Ge_2$ reveals only a single resonance mode corresponding to mode 2 in $EuSn_2As_2$ (see the Supplemental Material [40]). Hence, we conclude that mode 1 is characteristic of the axion-insulating phase as will be discussed below.

The temperature dependence for both geometries (static field within the easy plane but microwave field parallel and perpendicular to the easy plane) is shown in Fig. 3. On increasing temperature, the resonance fields of both resonance lines increase and finally merge in the paramagnetic phase. At higher temperatures, the ESR signal is well described by a single Dysonian. While at the lowest temperature the resonance field of the second mode is only weakly shifted from the paramagnetic resonance field, the first mode is found close to zero field.

In an easy-plane antiferromagnet, one expects two resonance modes dependent on the relative strength of external magnetic field H_0, exchange field H_E between the two sublattices, and anisotropy field H_A [44,45]. The anisotropy field H_A is determined from the difference between the critical fields required to align the moments along the c axis and in the ab plane at $T = 0$ K, i.e., $H_A = H_c^c - H_{ab}^c$. Taking into account the demagnetization factors to correct the critical field values H^c for the $2 \times 2 \times 0.5\,\mathrm{mm}^3$ crystal, we obtain $H_{ab}^c = H^c - 4\pi N_a M_s$ and $H_c^c = H^c - 4\pi N_c M_s$, where $N_a = 0.175$ and $N_c = 0.650$, which satisfy the relation $2N_a + N_c = 1$ [46,47]. M_s is the saturation magnetization. By substituting the values H^c and M_s for selected temperatures between 5 and 20 K from Ref. [38], the values of H_A decrease from 7.9 to 3 kOe. This must be compared to the antiferromagnetic exchange field between adjacent layers $H_E = 2|J_c|S/g\mu_B$, where $J_c \approx 0.32 \times 10^{-16}$ erg is the exchange constant along the c axis [48,49]. We obtain $H_E \approx 12$ kOe. Using these values, we can calculate the expected resonance positions. For $H_0 = 0$, one mode is found at $\omega = 0$, while the other exhibits an excitation gap $\omega = \gamma\sqrt{2H_E H_A}$ corresponding to a microwave frequency $\nu = \omega/(2\pi) \approx 39$ GHz. On application of $H_0 < 2H_E$ perpendicular to the plane, the lower mode remains an unobservable Goldstone mode at zero frequency, while the frequency of the upper mode monotonously increases approaching a linear field dependence. Thus, with our microwave frequency $\nu = 9.34$ GHz and the accessible magnetic field range $H < 18$ kOe, we do not expect any signal for this field geometry in agreement with our experimental observation. For the external field applied within the easy plane, the frequency of the lower mode increases linearly with the field following $\omega = \gamma H_0\sqrt{1 + H_A/(2H_E)}$, while the frequency of the upper mode gradually decreases, approaching zero at the spin-flop field $2H_E$. Under our experimental conditions, we can only observe the lower mode, which is expected to shift from $H_{res} = 3.12$ kOe in $T = 20$ K to $H_{res} = 2.70$ kOe in $T = 5$ K in fair agreement with the experimental data of the second mode.

The first mode at low field cannot be explained on the basis of the easy-plane antiferromagnet. It rather reminds us of the behavior expected for a thin ferromagnetic platelet. For the magnetic field applied within the plane, the resonance field is expected to shift to lower magnetic fields due to the demagnetization following $\omega = \gamma\sqrt{H(H + 4\pi M_s)}$. If the field is applied perpendicular to the plane, one expects $\omega = \gamma(H - 4\pi M_s)$ [50]. Using the resonance field $H = 0.6$ kOe observed at $T = 4.2$ K for the magnetic field applied within the ab plane, we determine a ferromagnetic saturation magnetization of $M_s = 1.4 \times 10^3$ emu/mol. Thus, for $H||c$ the ferromagnetic resonance signal is expected at about 21 kOe, which is beyond the field range of our electromagnet.

Previously, broadband magnetic resonance measurements of $EuSn_2As_2$ in the ab plane exhibited, besides the resonance close to the paramagnetic resonance field, the very same additional low-field resonance mode [51], which at 4 K is observable down to about $H_{res} \approx 0.6$ kOe at 9 GHz. It was speculated that magnetic point defects or stacking faults may be the origin of this additional resonance line. It was claimed that the presence of such defects may have a crucial effect on the magnetoresistance of the system such as abnormal Hall resistance, as was reported in Ref. [52]. Recent transmission electron microscopy investigations reveal ferromagnetic $EuSnAs_2$ layers within the $EuSn_2As_2$ matrix [53], which are stated to be responsible for the additional ferromagnetic resonance [54]. In this respect, we have to state that our samples do not reveal any indications of a ferromagnetic hysteresis for the magnetic field applied within the ab plane, as depicted in Fig. 10 of Ref. [38], in contrast to the samples described in Ref. [53]. Nevertheless, we observe the ferromagnetic-type resonance of comparable strength. Hence, taking into account the skin effect, we suggest that the ferromagnetic layers responsible for the observed resonance appear close to or directly at the surface and therefore are intimately connected to the axion-insulator characteristics of $EuSn_2As_2$ [26]. It is important to note that strong surface ferromagnetism was discovered earlier in the antiferromagnet $EuRh_2Si_2$ [55]. In this compound, formation of the surface ferromagnetism was attributed to the existence of surface states in an energy gap at the Fermi level.

For $T > T_N$, both the antiferromagnetic and the ferromagnetic resonance lines merge into a single line. Above 100 K, the linewidth ΔH is explained by the relaxation of the local-

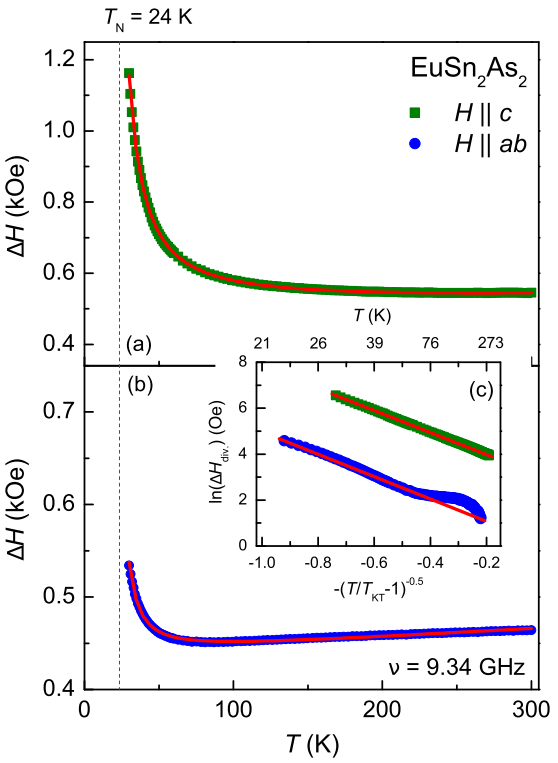

FIG. 4. (a), (b): Temperature dependence of the paramagnetic linewidth of $EuSn_2As_2$ measured at $\nu = 9.34$ GHz for applied magnetic field $H||c$ and $H||ab$, respectively. Solid lines represent the sum of Korringa relaxation and BKT scenario $\Delta H_K + \Delta H_{BKT} + \Delta H_0$, where ΔH_0 is the residual linewidth. The inset (c) shows the quality of the BKT fit using a logarithmic plot $\ln(\Delta H_{div})$ vs the reduced temperature $-(T/T_{KT} - 1)^{-0.5}$. The corresponding temperature values are depicted on the upper axis of the inset.

ized Eu^{2+} spins via scattering of the conduction electrons by Korringa's formula [56]:

$$\Delta H_K = \frac{\pi k_B}{g\mu_B}\langle J^2(q)\rangle D^2(E_F)T = \kappa T, \qquad (1)$$

where $\langle J^2(q)\rangle$ is the squared exchange constant between localized spins and conduction electrons averaged over the momentum transfer q, $D(E_F)$ is the conduction-electron density of states at Fermi energy E_F, and κ is the Korringa slope. For both $H||c$ and $H||ab$, $\kappa \approx 0.1$ Oe/K. This very small value shows that ΔH is nearly temperature independent [Figs. 4(a) and 4(b)]. The usual value of κ in Eu-based iron pnictides is between 6.5 and 8 Oe/K [57–61], which is typical of the S state of $4f^7$ local moments in conventional metals [62,63]. However, the absence of Korringa relaxation was reported in $EuIn_2As_2$ [64] and the highly ruthenium-doped $EuFe_{2-x}Ru_xAs_2$ [65]. It means that the conduction electrons are well separated from the localized Eu^{2+} spins. They are strongly confined within the SnAs layers. It suggests that at the europium site $D(E_F)$ nearly vanishes at the Fermi surface.

The anisotropy of ΔH at high temperatures exhibits the influence of the exchange-narrowed Eu^{2+} fine structure, suggesting the impact of crystalline electric-field effects [66]. The factor $g = h\nu/\mu_B H_{res.}$ remains nearly constant when the temperature increases to 300 K. Nevertheless, it lies slightly above the insulator value $g = 1.993$ of Eu^{2+}. The g anisotropy $\Delta g = g_{||ab} - g_{||c}$ is reduced by 12% when $T \to T_N$. The broadening of ΔH gives a hint to the development of antiferromagnetic short-range correlations. Below T_N, these correlations dominate the spin dynamics of Eu^{2+} spins and form pairs of topological magnetic defects (vortices) [41]. A topological phase transition can take place at T_{KT} [42,43]. The correlation length ξ is related to ΔH via [see Figs. 4(a) and 4(b)]

$$\Delta H_{BKT} = \Delta H_\infty \exp\left[3b/\sqrt{\frac{T}{T_{KT}} - 1}\right] \propto \xi^3, \qquad (2)$$

where ΔH_∞ is the ESR linewidth in the high-temperature approximation and $b = \pi/2$ for the square lattice [67]. This value, however, is also valid for other lattice geometries (see, e.g., Ref. [68]). The respective transition temperatures $T_{KT} \approx 11$ and ≈ 14 K for $H||c$ and $H||ab$ are around 45%–60% of T_N, which indicates that magnetic fluctuations extend deep into the ordered state as was already found in some frustrated antiferromagnetic oxides [69–71].

IV. CONCLUSION

In summary, we conducted antiferromagnetic resonance experiments on high-quality single crystals of $EuSn_2As_2$, which exhibit clear and robust surface and bulk magnon resonance modes in the ordered phase. Our findings show that the surface magnons are ferromagnons, which are only observed in the axion-insulating phase. They vanish as $T \to T_N$. The direct observation of these surface magnons could be a characteristic for the antiferromagnetic axion phase. On approaching the paramagnetic regime, both bulk magnon and surface magnon resonance lines merge into a single line at T_N. The analysis of the resultant linewidth ΔH obeys the BKT scenario, which proves both a two-dimensional and topological character of the Eu^{2+} spin system. At $T > 100$ K, the absence of Korringa relaxation proves the strong confinement of conduction electrons to the SnAs layers. This shows that the conduction electrons are well separated from the localized Eu^{2+} spins, which makes $EuSn_2As_2$ a true magnetic topological insulator.

ACKNOWLEDGMENTS

M.H. and H.-A.K.v.N. acknowledge funding by the Deutsche Forschungsgemeinschaft (DFG) within the Transregional Collaborative Research Center TRR 360 "Constrained Quantum Matter," Project No. 492547816 (Augsburg, Munich, Stuttgart, Leipzig). The research at Ames National Laboratory was supported by the U.S. Department of Energy, Office of Basic Energy Sciences, Division of Materials Sciences and Engineering. Ames National Laboratory is operated for the U.S. Department of Energy by Iowa State University under Contract No. DE-AC02-07CH11358.

[1] R. D. Peccei and Helen R. Quinn, CP conservation in the presence of pseudoparticles, Phys. Rev. Lett. **38**, 1440 (1977).

[2] R. D. Peccei and Helen R. Quinn, Constraints imposed by CP conservation in the presence of pseudoparticles, Phys. Rev. D **16**, 1791 (1977).

[3] S. Weinberg, A new light boson? Phys. Rev. Lett. **40**, 223 (1978).

[4] F. Wilczek, Problem of strong P and T invariance in the presence of instantons, Phys. Rev. Lett. **40**, 279 (1978).

[5] E. Fradkin, E. Dagotto, and D. Boyanovsky, Physical realization of the parity anomaly in condensed matter physics, Phys. Rev. Lett. **57**, 2967 (1986).

[6] F. Wilczek, Two applications of axion electrodynamics, Phys. Rev. Lett. **58**, 1799 (1987).

[7] R. Li, J. Wang, X.-L. Qi, and S.-C. Zhang, Dynamical axion field in topological magnetic insulators, Nat. Phys. **6**, 284 (2010).

[8] T. Kurumaji, Y. Takahashi, J. Fujioka, R. Masuda, H. Shishikura, S. Ishiwata, and Y. Tokura, Optical magnetoelectric resonance in a polar magnet $(Fe, Zn)_2Mo_3O_8$ with axion-type coupling, Phys. Rev. Lett. **119**, 077206 (2017).

[9] A. M. Essin, J. E. Moore, and D. Vanderbilt, Magnetoelectric polarizability and axion electrodynamics in crystalline insulators, Phys. Rev. Lett. **102**, 146805 (2009).

[10] R. S. K. Mong, A. M. Essin, and J. E. Moore, Antiferromagnetic topological insulators, Phys. Rev. B **81**, 245209 (2010).

[11] Y. Tokura, K. Yasuda, and A. Tsukazaki, Magnetic topological insulators, Nat. Rev. Phys. **1**, 126 (2019).

[12] K. M. Fijalkowski, N. Liu, M. Hartl, M. Winnerlein, P. Mandal, A. Coschizza, A. Fothergill, S. Grauer, S. Schreyeck, K. Brunner, M. Greiter, R. Thomale, C. Gould, and L. W. Molenkamp, Any axion insulator must be a bulk three-dimensional topological insulator, Phys. Rev. B **103**, 235111 (2021).

[13] V. Bonbien, F. Zhuo, A. Salimath, O. Ly, A. Abbout, and A. Manchon, Topological aspects of antiferromagnets, J. Phys. D: Appl. Phys. **55**, 103002 (2022).

[14] A. Sekine and K. Nomura, Axion electrodynamics in topological materials, J. Appl. Phys. **129**, 141101 (2021).

[15] J.-Q. Yan, Q. Zhang, T. Heitmann, Zengle Huang, K. Y. Chen, J.-G. Cheng, Weida Wu, D. Vaknin, B. C. Sales, and R. J. McQueeney, Crystal growth and magnetic structure of $MnBi_2Te_4$, Phys. Rev. Mater. **3**, 064202 (2019).

[16] M. M. Otrokov, I. P. Rusinov, M. Blanco-Rey, M. Hoffmann, A. Yu Vyazovskaya, S. V. Eremeev, A. Ernst, P. M. Echenique, A. Arnau, and E. V. Chulkov, Unique thickness-dependent properties of the van der Waals interlayer antiferromagnet $MnBi_2Te_4$ films, Phys. Rev. Lett. **122**, 107202 (2019).

[17] Y. J. Chen, L. X. Xu, J. H. Li, Y. W. Li, H. Y. Wang, C. F. Zhang, H. Li, Y. Wu, A. J. Liang, C. Chen, S. W. Jung, C. Cacho, Y. H. Mao, S. Liu, M. X. Wang, Y. F. Guo, Y. Xu, Z. K. Liu, L. X. Yang, and Y. L. Chen, Topological electronic structure and its temperature evolution in antiferromagnetic topological insulator $MnBi_2Te_4$, Phys. Rev. X **9**, 041040 (2019).

[18] Y.-J. Hao, P. Liu, Y. Feng, X.-M. Ma, E. F. Schwier, M. Arita, S. Kumar, C. Hu, R. Lu, M. Zeng, *et al.*, Gapless surface Dirac cone in antiferromagnetic topological insulator $MnBi_2Te_4$, Phys. Rev. X **9**, 041038 (2019).

[19] C. Liu, Y. Wang, H. Li, Y. Wu, Y. Li, J. Li, K. He, Y. Xu, J. Zhang, and Y. Wang, Robust axion insulator and Chern insulator phases in a two-dimensional antiferromagnetic topological insulator, Nat. Mater. **19**, 522 (2020).

[20] A. Alfonsov, J. I. Facio, K. Mehlawat, A. G. Moghaddam, R. Ray, A. Zeugner, M. Richter, J. van den Brink, A. Isaeva, B. Büchner, and V. Kataev, Strongly anisotropic spin dynamics in magnetic topological insulators, Phys. Rev. B **103**, L180403 (2021).

[21] T. Zhu, H. Wang, H. Zhang, and D. Xing, Tunable dynamical magnetoelectric effect in antiferromagnetic topological insulator $MnBi_2Te_4$ films, npj Comp. Mater. **7**, 121 (2021).

[22] A. M. Shikin, D. A. Estyunin, D. A. Glazkova, S. O. Fil'nov, and I. I. Klimovskikh, Electronic and spin structures of intrinsic antiferromagnetic topological insulators of the $MnBi_2Te_4(Bi_2Te_3)_m$ family and their magnetic properties, JETP Lett. **115**, 213 (2022).

[23] H. Li, S.-Y. Gao, S.-F. Duan, Y.-F. Xu, K.-J. Zhu, S.-J. Tian, J.-C. Gao, W.-H. Fan, Z.-C. Rao, J.-R. Huang, *et al.*, Dirac surface states in intrinsic magnetic topological insulators $EuSn_2As_2$ and $MnBi_{2n}Te_{3n+1}$, Phys. Rev. X **9**, 041039 (2019).

[24] J. Zhang, D. Wang, M. Shi, T. Zhu, H. Zhang, and J. Wang, Large dynamical axion field in topological antiferromagnetic insulator $Mn_2Bi_2Te_5$, Chin. Phys. Lett. **37**, 077304 (2020).

[25] Y. Li, Y. Jiang, J. Zhang, Z. Liu, Z. Yang, and J. Wang, Intrinsic topological phases in $Mn_2Bi_2Te_5$ tuned by the layer magnetization, Phys. Rev. B **102**, 121107(R) (2020).

[26] M. Gu, J. Li, H. Sun, Y. Zhao, C. Liu, J. Liu, H. Lu, and Q. Liu, Spectral signatures of the surface anomalous Hall effect in magnetic axion insulators, Nat. Commun. **12**, 3524 (2021).

[27] G. Naselli, A. G. Moghaddam, S. D. Napoli, V. Vildosola, I. C. Fulga, J. van den Brink, and J. I. Facio, Magnetic warping in topological insulators, Phys. Rev. Res. **4**, 033198 (2022).

[28] A. B. Sarkar, S. Mardanya, S.-M. Huang, B. Ghosh, C.-Y. Huang, H. Lin, A. Bansil, T.-R. Chang, A. Agarwal, and B. Singh, Magnetically tunable Dirac and Weyl fermions in the Zintl materials family, Phys. Rev. Mater. **6**, 044204 (2022).

[29] A. M. Goforth, P. Klavins, J. C. Fettinger, and S. M. Kauzlarich, Magnetic properties and negative colossal magnetoresistance of the rare earth Zintl phase $EuIn_2As_2$, Inorg. Chem. **47**, 11048 (2008).

[30] S. X. M. Riberolles, T. V. Trevisan, B. Kuthanazhi, T. W. Heitmann, F. Ye, D. C. Johnston, S. L. Bud'ko, D. H. Ryan, P. C. Canfield, A. Kreyssig, A. Vishwanath, R. J. McQueeney, L.-L. Wang, P. P. Orth, and B. G. Ueland, Magnetic crystalline-symmetry-protected axion electrodynamics and field-tunable unpinned Dirac cones in $EuIn_2As_2$, Nat. Commun. **12**, 999 (2021).

[31] M. Gong, D. Sar, J. Friedman, D. Kaczorowski, S. Abdel Razek, W.-C. Lee, and P. Aynajian, Surface state evolution induced by magnetic order in axion insulator candidate $EuIn_2As_2$, Phys. Rev. B **106**, 125156 (2022).

[32] J. Yan, Z. Z. Jiang, R. C. Xiao, W. J. Lu, W. H. Song, X. B. Zhu, X. Luo, Y. P. Sun, and M. Yamashita, Field-induced topological Hall effect in antiferromagnetic axion insulator candidate $EuIn_2As_2$, Phys. Rev. Res. **4**, 013163 (2022).

[33] Q. Wu, T. Hu, D. Wu, R. Li, L. Yue, S. Zhang, S. Xu, Q. Liu, T. Dong, and N. Wang, Spin dynamics in the axion insulator candidate $EuIn_2As_2$, Phys. Rev. B **107**, 174411 (2023).

[34] J.-R. Soh, A. Bombardi, F. Mila, M. C. Rahn, D. Prabhakaran, S. Francoual, H. M. Rønnow, and A. T. Boothroyd, Understanding unconventional magnetic order in a candidate axion

insulator by resonant elastic x-ray scattering, Nat. Commun. **14**, 3387 (2023).

[35] G. M. Pierantozzi, A. D. Vita, C. Bigi, X. Gui, H. -j. Tien, D. Mondal, F. Mazzola, J. Fujii, I. Vobornik, G. Vinai, A. Sala, C. Africh, T.-L. Lee, G. Rossi, T.-R. Chang, W. Xie, R. J. Cava, G. Panaccione, Evidence of magnetism-induced topological protection in the axion insulator candidate $EuSn_2P_2$, Proc. Natl. Acad. Sci. USA **119**, e2116575119 (2022).

[36] X. Yang, J. Pan, X. He, L. Cao, Y. Cao, and Y. Tao, Three-dimensional critical behavior and anisotropic magnetic entropy change in the axion insulator candidate $EuSn_2P_2$, Phys. Rev. B **107**, 054440 (2023).

[37] M. Q. Arguilla, N. D. Cultrara, Z. J. Baum, S. Jiang, R. D. Ross, and J. E. Goldberger, $EuSn_2As_2$: An exfoliatable magnetic layered Zintl-Klemm phase, Inorg. Chem. Front. **4**, 378 (2017).

[38] S. Pakhira, M. A. Tanatar, T. Heitmann, D. Vaknin, and D. C. Johnston, *A*-type antiferromagnetic order and magnetic phase diagram of the trigonal Eu spin-$\frac{7}{2}$ triangular-lattice compound $EuSn_2As_2$, Phys. Rev. B **104**, 174427 (2021).

[39] X. Lv, X. Chen, B. Zhang, P. Jiang, and Z. Zhong, Thickness-dependent magnetism and topological properties of $EuSn_2As_2$, ACS Appl. Electron. Mater. **4**, 3212 (2022).

[40] See Supplemental Material at http://link.aps.org/supplemental/10.1103/dp4g-dyll for revealing magnetization and low-temperature ($4 \leqslant T \leqslant 30$ K) ESR data of the isostructural reference compound $EuAl_2Ge_2$, which possesses very similar exchange interactions and anisotropy of $EuSn_2As_2$, but is classified as conventional topological insulator without axion phase. Comparisons are depicted between ESR-parameters (i.e.: resonance field, linewidth, and intensity) of both $EuSn_2As_2$ and $EuAl_2Ge_2$.

[41] V. Berezinskii, Destruction of long-range order in one-dimensional and two-dimensional systems possessing a continuous symmetry group, II. Quantum Systems, Zh. Eksp. Teor. Fiz, **61**, 610 (1972); Zh. Eksp. Teor. Fiz. **61**, 1144 (1971).

[42] J. M. Kosterlitz and D. J. Thouless, Ordering, metastability and phase transitions in two-dimensional systems, J. Phys. C **6**, 1181 (1973).

[43] J. M. Kosterlitz, The critical properties of the two-dimensional XY model, J. Phys. C **7**, 1046 (1974).

[44] A. G. Gurevich and G. A. Melkov, *Magnetization Oscillations and Waves* (CRC Press, Boca Raton, FL, 1996).

[45] S. M. Rezende, *Fundamentals of Magnonics*, 1st ed., Lecture Notes of Physics, Vol. 969 (Springer, Berlin, 2020).

[46] A. Aharoni, Demagnetizing factors for rectangular ferromagnetic prisms, J. Appl. Phys. **83**, 3432 (1998).

[47] D. C. Johnston, Magnetic dipole interactions in crystals, Phys. Rev. B **93**, 014421 (2016).

[48] D. C. Johnston, Unified molecular field theory for collinear and noncollinear Heisenberg antiferromagnets, Phys. Rev. B **91**, 064427 (2015).

[49] S. Pakhira, F. Islam, E. O'Leary, M. A. Tanatar, T. Heitmann, L.-L. Wang, R. Prozorov, A. Kaminski, D. Vaknin, and D. C. Johnston, A-type antiferromagnetic order in semiconducting $EuMg_2Sb_2$ single crystals, Phys. Rev. B **106**, 024418 (2022).

[50] Ch Kittel, On the theory of ferromagnetic resonance absorption, Phys. Rev. **73**, 155 (1948).

[51] I. A. Golovchanskiy, E. I. Maltsev, I. V. Shchetinin, V. A. Vlasenko, P. S. Dzhumaev, K. Pervakov, O. V. Emelyanova, A. Yu Tsvetkov, N. N. Abramov, V. M. Pudalov, and V. S. Stolyarov, Magnetic resonances in $EuSn_2As_2$ single crystal, J. Magn. Magn. Mater. **562**, 169713 (2022).

[52] H. Li, W. Gao, Z. Chen, W. Chu, Y. Nie, S. Ma, Y. Han, M. Wu, T. Li, Q. Niu, W. Ning, X. Zhu, and M. Tian, Magnetic properties of the layered magnetic topological insulator $EuSn_2As_2$, Phys. Rev. B **104**, 054435 (2021).

[53] A. Yu Levakhova, A. L. Vasiliev, N. S. Pavlov, A. V. Ovcharov, V. I. Bondarenko, A. V. Sadakov, K. S. Pervakov, V. A. Vlasenko, and V. M. Pudalov, Emergence of ferromagnetism from planar defects in $EuSn_2As_2$ antiferromagnet, arXiv:2511.03582.

[54] I. I. Gimazov, D. E. Zhelezniakova, R. B. Zaripov, Yu I. Talanov, A. Yu Levakhova, A. V. Sadakov, K. S. Pervakov, V. A. Vlasenko, A. L. Vasiliev, and V. M. Pudalov, Ferromagnetic resonance in an antiferromagnetic crystal $EuSn_2As_2$, arXiv:2512.13571.

[55] A. Chikina, M. Höppner, S. Seiro, K. Kummer, S. Danzenbächer, S. Patil, A. Generalov, M. Güttler, Yu Kucherenko, E. V. Chulkov, Yu M. Koroteev, K. Köpernik, C. Geibel, M. Shi, M. Radovic, C. Laubschat, and D. V. Vyalikh, Strong ferromagnetism at the surface of an antiferromagnet caused by buried magnetic moments, Nat. Commun. **5**, 3171 (2014).

[56] J. Korringa, Nuclear magnetic relaxation and resonance line shift in metals, Physica **16**, 601 (1950).

[57] E. Dengler, J. Deisenhofer, H.-A. Krug von Nidda, Seunghyun Khim, J. S. Kim, Kee Hoon Kim, F. Casper, C. Felser, and A. Loidl, Strong reduction of the Korringa relaxation in the spin-density wave regime of $EuFe_2As_2$ observed by electron spin resonance, Phys. Rev. B **81**, 024406 (2010).

[58] J. J. Ying, T. Wu, Q. J. Zheng, Y. He, G. Wu, Q. J. Li, Y. J. Yan, Y. L. Xie, R. H. Liu, X. F. Wang, and X. H. Chen, Electron spin resonance in $EuFe_{2-x}Co_xAs_2$ single crystals, Phys. Rev. B **81**, 052503 (2010).

[59] N. Pascher, J. Deisenhofer, H.-A. Krug von Nidda, M. Hemmida, H. S. Jeevan, P. Gegenwart, and A. Loidl, Magnetic fluctuations and superconductivity in iron pnictides as probed by electron spin resonance, Phys. Rev. B **82**, 054525 (2010).

[60] H.-A. Krug von Nidda, S. Kraus, S. Schaile, E. Dengler, N. Pascher, M. Hemmida, M. J. Eom, J. S. Kim, H. S. Jeevan, P. Gegenwart, J. Deisenhofer, and A. Loidl, Electron spin resonance in Eu-based iron pnictides, Phys. Rev. B **86**, 094411 (2012).

[61] F. A. Garcia, A. Leithe-Jasper, W. Schnelle, M. Nicklas, H. Rosner, and J. Sichelschmidt, Field dependence of the Eu^{2+} spin relaxation in $EuFe_{2-x}Co_xAs_2$, New J. Phys. **14**, 063005 (2012).

[62] R. H. Taylor, Electron spin resonance of magnetic ions in metals: An experimental review, Adv. Phys. **24**, 681 (1975).

[63] S. Barnes, Theory of electron spin resonance of magnetic ions in metals, Adv. Phys. **30**, 801 (1981).

[64] P. F. S. Rosa, C. Adriano, T. M. Garitezi, R. A. Ribeiro, Z. Fisk, and P. G. Pagliuso, Electron spin resonance of the intermetallic antiferromagnet $EuIn_2As_2$, Phys. Rev. B **86**, 094408 (2012).

[65] M. Hemmida, H.-A. Krug von Nidda, A. Günther, A. Loidl, A. Leithe-Jasper, W. Schnelle, H. Rosner, and J. Sichelschmidt,

Probing the density of states in $EuFe_{2-x}Ru_xAs_2$, Phys. Rev. B **90**, 205105 (2014).

[66] G. Lacueva, P. M. Levy, and A. Fert, Crystal field of Gd^{3+} in hexagonal metals, Phys. Rev. B **31**, 6245 (1985).

[67] M. Hemmida, N. Winterhalter-Stocker, D. Ehlers, H.-A. Krug von Nidda, M. Yao, J. Bannies, E. D. L. Rienks, R. Kurleto, C. Felser, B. Büchner, J. Fink, S. Gorol, T. Förster, S. Arsenijevic, V. Fritsch, and P. Gegenwart, Topological magnetic order and superconductivity in $EuRbFe_4As_4$, Phys. Rev. B **103**, 195112 (2021).

[68] M. Heinrich, H.-A. Krug von Nidda, A. Loidl, N. Rogado, and R. J. Cava, Potential signature of a Kosterlitz-Thouless transition in $BaNi_2V_2O_8$, Phys. Rev. Lett. **91**, 137601 (2003).

[69] M. Hemmida, H.-A. Krug von Nidda, N. Büttgen, A. Loidl, L. K. Alexander, R. Nath, A. V. Mahajan, R. F. Berger, R. J. Cava, Y. Singh, and D. C. Johnston, Vortex dynamics and frustration in two-dimensional triangular chromium lattices, Phys. Rev. B **80**, 054406 (2009).

[70] M. Hemmida, H.-A. Krug von Nidda, and A. Loidl, Traces of Z_2-vortices in $CuCrO_2$, $AgCrO_2$, and $PdCrO_2$, J. Phys. Soc. Jpn. **80**, 053707 (2011).

[71] M. Hemmida, H.-A. Krug von Nidda, V. Tsurkan, and A. Loidl, Berezinskii-Kosterlitz-Thouless type scenario in the molecular spin liquid ACr_2O_4 (A = Mg, Zn, Cd), Phys. Rev. B **95**, 224101 (2017).